X-ray-absorption spectroscopy at the Fe $L_{2,3}$ threshold in iron oxides

J. P. Crocombette, M. Pollak, F. Jollet, N. Thromat, and M. Gautier-Soyer
Commissariat à l'Energie Atomique, Direction des Sciences de la Matière, Département de Recherche sur l'Etat Condensé les Atomes et les Molecules, Service de Recherche sur les Surfaces et l'Irradiation de la Matière, Centre d'Etudes de Saclay, Bâtiment 462, 91191 Gif-sur-Yvette CEDEX, France
(Received 21 November 1994)

The influence of local order around the iron site on Fe $2p$ x-ray-absorption spectra is studied for α-Fe_2O_3, FeO, Fe_3O_4, and γ-Fe_2O_3. The experimental spectra are accounted for thanks to a configuration-interaction calculation of Fe $L_{2,3}$ x-ray-absorption edge shapes, explicitly taking into account the exact first-neighbor surrounding of the cation acting through crystal-field splitting and hopping terms. The peak's splittings and intensities are well reproduced: the contributions of the various iron site symmetries and valencies are discriminated. The nature of insulating gap for each compound is deduced.

I. INTRODUCTION

Iron oxides have a great importance in many technological fields, as catalysis or data storage[1,2] and have therefore widely been studied this last decade. Indeed, they present an interesting variety of properties from a structural point of view as well as from an electronic, magnetic, or chemical one. Among them, α-Fe_2O_3 is an antiferromagnetic insulator with a corrundum structure in which the iron sites are nearly perfect octahedra with formally Fe^{3+} ions; γ-Fe_2O_3 and Fe_3O_4 are ferrimagnetic compounds with inverse spinel structure in which the iron sites are distorted octahedra and tetrahedra with formally Fe^{3+} ions for the first one and distorted octahedra and tetrahedra with formally Fe^{3+} and Fe^{2+} ions for the last one. The latter is a semiconductor while the former is an insulator. At last, FeO is an antiferromagnetic insulator which has ideally a NaCl structure in which the Fe^{2+} sites are octahedral. The iron sites in iron oxides present therefore a variety of local environments (perfect or distorted octahedra or tetrahedra) associated with two possible iron valencies (2+ and 3+) so that it proves necessary to have a local structural and electronic probe to discriminate the different sites.

This is the case with the Fe electron energy loss spectroscopy (EELS) and x-ray-absorption spectroscopy (XAS) edges, that are known to be very sensitive to local order.[3] The most abundant experimental data have been obtained by EELS: Colliex *et al.* have studied the four iron oxides at the K oxygen edge and at the $L_{2,3}$ iron edge, but the experimental resolution does not enable one to clearly distinguish the Fe $L_{2,3}$ spectra of the different phases;[4] Paterson and Krivanek show nice high-resolution spectra of the Fe $L_{2,3}$ edge in α-Fe_2O_3, γ-Fe_2O_3, and Fe_3O_4,[5] while the Fe $L_{2,3}$ edge in FeO was published in Ref. 6. It is suggested in Ref. 7 that the L_3 spectrum for Fe_3O_4 has three components coming from octahedral and tetrahedral Fe^{3+} sites and from the octahedral Fe^{2+} sites. In what concerns XAS, van der Laan *et al.* have obtained, among different iron compounds, the Fe $2p$ edges of α-Fe_2O_3 and Fe_3O_4.[8] Studying x-ray magnetic dichroism of Fe_2O_3, Kuiper *et al.* show also a very well-resolved spectrum of the Fe $L_{2,3}$ edge of α-Fe_2O_3.[9] On the theoretical side, calculations have been performed in the frame of the ionic multiplet ligand field theory on perfect FeO_6 octahedra:[9,10] it is concluded that the $2p$-core-hole–d-electron multiplet interactions are responsible for the whole shape of the spectrum. To our knowledge, there are no similar calculations for the other iron oxides in the literature; moreover, it is not clear at the moment how important the charge-transfer effects are that are neglected in the ionic multiplet model.

In this paper, we present a systematic study of the contribution of each iron site to the Fe $L_{2,3}$ edge in the four iron oxides. For this, we show Fe $L_{2,3}$ XAS experimental spectra of α-Fe_2O_3, Fe_3O_4, and FeO together with calculations of the excitation spectra at the Fe $L_{2,3}$ edge for all the iron sites encountered in α-Fe_2O_3, γ-Fe_2O_3, Fe_3O_4, and FeO. This is done thanks to a configuration interaction calculation explicitly taking into account the exact first-neighbor surrounding of the cation acting through crystal-field splitting and hopping terms. Sample preparation and experimental conditions are presented in Sec. II while Sec. III is devoted to the calculation method. In Sec. IV, we show the experimental results and investigate the respective influence of the site symmetry and of the cation valency on the spectral shape of the four oxides. We end by discussing the nature of the insulating gap in these oxides according to the ZSA classification.[11]

II. EXPERIMENTAL

The hematite (α-Fe_2O_3) sample was synthesized by Remeika (AT&T Bell Laboratories) using the flux method (Bi_2O_3, B_2O_3). It exhibits a natural growth face having a $(10\bar{1}2)$ orientation, as determined by Laue x-ray diffraction. Fe_3O_4 (magnetite) and FeO (wüstite) single crystals, grown by the zone fusion method, were provided by the Laboratoire de Chimie des Solides (Orsay, France). A sample of Fe_3O_4 was cut along a (111) plane and FeO along (100), and polished. Prior to their loading in the preparation chamber, they were cleaned ultrasonically in ethanol. No *in situ* cleaning or checking of the samples

0163-1829/95/52(5)/3143(8)/$06.00

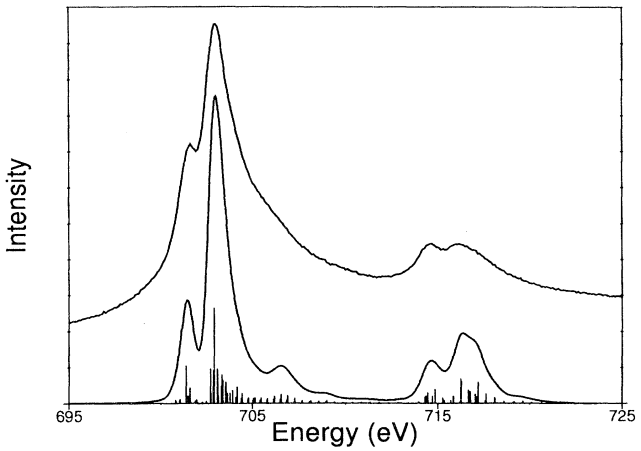

FIG. 1. Theoretical and experimental Fe $2p$ x-ray-absorption edge in α-Fe_2O_3. The upper solid line indicates the experimental spectrum, the lower solid line is the calculation, the vertical bars are poles of the theoretical spectrum.

was performed so that the presence of other oxidation states at the surface cannot be excluded.

X-ray-absorption experiments were carried out on the SA 72 beam line of Super ACO at the LURE-Orsay synchrotron facilities. The preparation chamber allows base pressure down to 5×10^{-11} mbar. A toroidal grating mirror monochromator (TGM) supplies an incident photon beam with energies ranging from 150 to 900 eV. The total electron yield (I) was measured by a channeltron placed in front of the irradiated sample. The primary photon beam intensity (I_0) was monitored by a second channeltron, which measures the total electron current from a gold grid located in front of the analysis chamber in the path of the photon beam. The I/I_0 ratio was measured as a function of photon energy, ranging from 684 to 744 eV, with a resolution of 0.9 eV. In Figs. 1–3, the experimental spectra have been normalized with respect to the background so that, before the absorption edge, it is equal to 0 and after the absorption edge (724 eV) it is equal to 1.

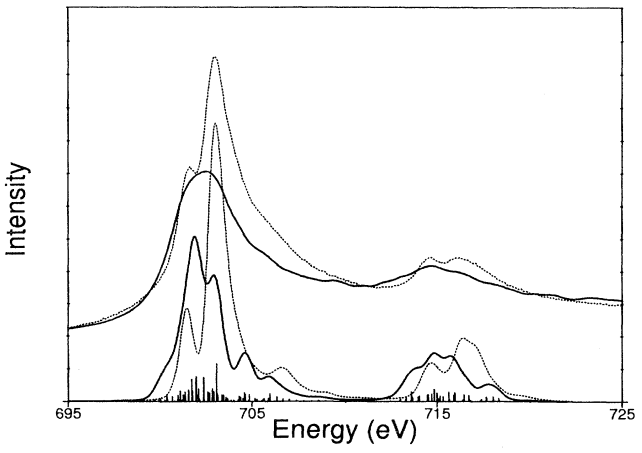

FIG. 2. Theoretical and experimental Fe $2p$ x-ray-absorption edge in FeO. The upper solid line indicates the experimental spectrum, the lower solid line is the calculation, the vertical bars are poles of the theoretical spectrum. In the dashed lines are figured the theoretical (bottom) and experimental (top) spectra of α-Fe_2O_3 for comparison.

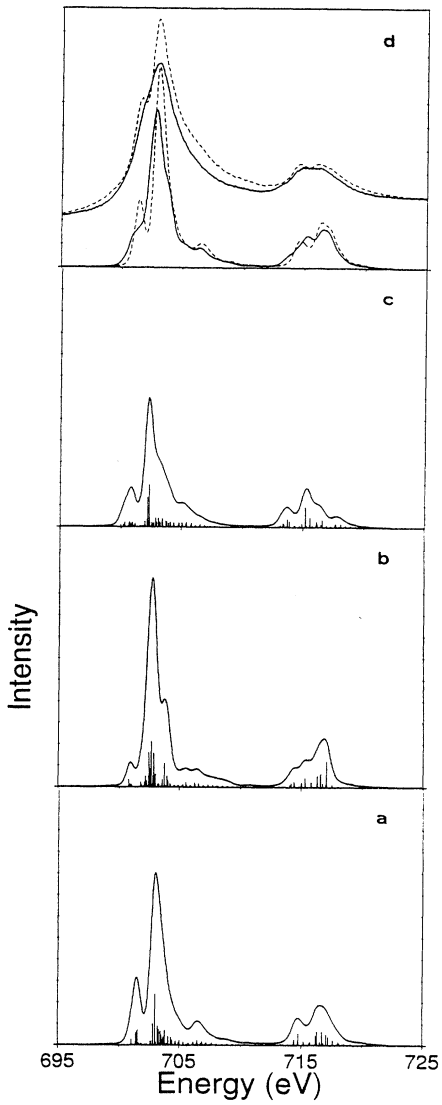

FIG. 3. Theoretical and experimental Fe $2p$ x-ray-absorption edge in Fe_3O_4. (a) Theoretical spectrum and poles of the octahedral Fe^{3+} site. (b) Theoretical spectrum and poles of the tetrahedral Fe^{3+} site. (c) Theoretical spectrum and poles of the octahedral Fe^{2+} site. (d) Upper solid line indicates the experimental Fe_3O_4 spectrum, the lower solid line is the theoretical Fe_3O_4 spectrum obtained by summation of (a)–(c). In the dashed lines are figured the theoretical (bottom) and experimental (top) spectra of α-Fe_2O_3 for comparison.

III. CALCULATION METHOD

It is known that, in transition-metal oxides, cation-$2p$ XAS is dominated by intra-atomic and short-range

effects.[3] In view of this, the basic object of the model is a cluster made of a central iron cation surrounded by its oxygen first neighbors. The ions are in exact positions relative to each other. The $2p$ orbitals of the oxygen atoms and the d and $2p$ orbitals of the cation are considered. Configurations with more than one ligand hole in the oxygen $2p$ orbitals have been neglected in the calculations. The Hamiltonian of the system takes into account the charge transfer (through hopping terms), the crystal-field splitting, the intracationic electronic repulsions (i.e., d electron interactions and electron–core-hole interactions) and spin-orbit coupling of $2p$ orbitals of the cation. Spin-orbit coupling of valence orbitals (oxygen $2p$ and cation d) have been neglected. Crystal-field calculation is explained in Ref. 12. The Hamiltonian of the cluster is written out in a basis of Slater determinants. Details about the way it is calculated can be found elsewhere.[13]

The Slater integrals F^2_{dd}, F^4_{dd}, F^2_{pd}, G^1_{pd}, and G^3_{pd} controlling the multiplet splitting on the cation have been taken from *ab initio* Hartree-Fock calculations,[3] but these values obtained by a monoelectronic method should be reduced to account for intra-atomic correlation effects before use in CI calculations.[14] We chose a multiplicative factor of 80%. The spin-orbit coupling parameters are taken from the same Hartree-Fock calculations[3] but no reduction coefficient was applied on them.

The $2p$ XAS spectrum is dominated by dipole-allowed transitions to d and s final states. Due to larger wave-function overlap the d channel is much stronger than the s one.[15] Subsequently the latter is neglected. Core-hole intrinsic lifetime broadenings as tabulated in Ref. 16 (i.e., 0.2 eV for L_3 and 0.37 eV for L_2 edges, respectively) have been used. A supplementary convolution with a Gaussian broadening (0.6 eV) is applied to account for experimental resolution.

The parameters used in the calculation to fit the experimental spectra are the following.

(1) $\overline{r^2}$ and $\overline{r^4}$ for crystal-field splittings leading to the ϵ_δ crystal-field energy of the orbitals as explained in Ref. 12. It must be stressed here that within this approach, only these two parameters are necessary to obtain the eigenvalues and eigenvectors of the crystal field, whatever the local order around the cation may be.

(2) η_σ which is the multiplicative factor in Harrison's formulas for hopping terms.[17] This parameter pilots the hopping terms from oxygen to cation d orbitals.

(3) $\Delta_\epsilon = \epsilon_d - \epsilon_p$ measuring the difference in energy of cation d and oxygen $2p$ orbitals.

(4) F^0_{pd} and F^0_{dd} which are the isotropic attraction of the final-state $2p$ core hole on the d electrons and isotropic d-d electronic repulsion.

With a set of values for the parameters, the difference between the lowest d^n and $d^{n+1}\underline{L}$ configurations energies can be calculated (n being the formal number of d electrons in the ionic configuration). This quantity is denoted Δ. Its formal expression depends on n and on the high or low spin state of the cation.[18] In the next section, we consider the cases of a high-spin d^5 ion in an octahedral or tetrahedral site and of a high-spin d^6 ion in an octahedral site that occurs in iron oxides. For these cases the formal expressions of Δ are

$$\text{octahedral } d^5\text{: } \Delta = 5F^0_{dd} + \Delta_\epsilon - 4Dq \ ,$$

$$\text{tetrahedral } d^5\text{: } \Delta = 5F^0_{dd} + \Delta_\epsilon - 6Dq \ ,$$

$$\text{octahedral } d^6\text{: } \Delta = 6F^0_{dd} - \tfrac{5}{49}F^2_{dd} - \tfrac{8}{147}F^4_{dd} + \Delta_\epsilon - 4Dq \ .$$

In the following we deal with the cases of α-Fe_2O_3, FeO, Fe_3O_4, and γ-Fe_2O_3 successively. We used crystallographic structure data from Ref. 19 and also Ref. 20 for γ-Fe_2O_3.

IV. RESULTS AND DISCUSSION

A. α-Fe_2O_3

In the case of α-Fe_2O_3 all the iron sites are equivalent. The iron ions occupy octahedral sites very slightly distorted from perfect O_h symmetry (see Table I for iron oxygen distances). Their valency is Fe^{3+} leading to formally d^5 configuration. So the calculation of the iron $L_{2,3}$ edge shape for this oxide involves only one FeO_6 cluster.

The charge-transfer parameters (Δ_ϵ, η_σ, F^0_{pd}, and F^0_{dd}) were obtained from a fit of cation $2p$ x-ray photoelectron spectroscopy (XPS) in α-Fe_2O_3. Indeed, our code enables us to simulate cation $2p$ XAS and also cation $2p$ XPS. The experimental $2p$ XPS spectrum of α-Fe_2O_3 presents two peaks due to $2p$ spin-orbit coupling and two satellites 8.2 eV distant from the main peaks and having an intensity of about 10% of the main ones. It is now admitted that these satellites are attributed to charge-transfer processes in the final state because of the core-hole attraction on d orbitals.[21] We decided to fix our parameters Δ_ϵ, η_σ, F^0_{pd}, and F^0_{dd} (all acting on charge transfer) so as to reproduce the experimental $2p$ XPS. The other parameters $\overline{r^2}$ and $\overline{r^4}$ were not considered in the fit as they have, in a first approach, little influence on the spectral XPS shape. They were fitted so as to reproduce the $L_{2,3}$ edge of iron in α-Fe_2O_3. The values obtained are given in Table II. The configuration energy difference in α-Fe_2O_3, including the calculated crystal field, is $\Delta = E(d^6\underline{L}) - E(d^5) = 2.2$ eV.

The experimental and theoretical spectra are given in Fig. 1. The theoretical spectrum has been normalized to the experimental spectrum so that L_3 main peaks have the same intensity. Once determined for α-Fe_2O_3, the same normalization coefficients have been used for all other oxides considered hereafter, i.e., the theoretical spectra were multiplied by the same quantity. The agreement is quite good: due to iron $2p$ spin-orbit coupling the spectra are divided in two parts corresponding to the L_3 and L_2 edges. Both these edges are divided in two peaks. The splittings and intensity ratios between these two peaks come from the interplay of crystal-field ($10Dq = 0.88$ eV) and electronic interactions[10] and cannot be directly related to the division of d orbitals in t_{2g} and e_g subsets. The approximate weight of the ground-state $d^6\underline{L}$ configuration (given in Table III) is quite important showing the importance of charge transfer in this materi-

TABLE I. Iron-oxygen distances and approximate site symmetry in iron oxides [for γ-Fe_2O_3 the number of iron of each site for the conventional small lattice (Ref. 20) is also indicated].

α-Fe_2O_3 Octahedral site	FeO Octahedral site	Fe_3O_4 Tetrahedral site	Fe_3O_4 Octahedral site	γ-Fe_2O_3 Tetrahedral site	γ-Fe_2O_3 Octahedral site	γ-Fe_2O_3 Octahedral site	γ-Fe_2O_3 Octahedral site
1.91 (×3)	2.15 (×6)	1.87 (×4)	2.07 (×6)	1.86 (×2)	2.08 (×2)	2.10 (×2)	1.99 (×2)
2.06 (×3)				1.88 (×1)	2.04 (×2)	2.11 (×1)	2.33 (×2)
				1.92 (×1)	1.98 (×2)	1.90 (×1)	2.06 (×2)
						1.92 (×1)	
						1.98 (×1)	
				×8	×4	×8	×4/3

al. Charge transfer has two main effects on spectral shape. First, it reinforces the splitting of d orbitals by the formation of molecular orbitals more splitted than the atomic ones. So neglecting it causes an overestimation of crystal-field splittings. Second, charge transfer acts on the shape of the tails that can be seen on the higher-energy side of the edges, especially the L_3 one. Ionic calculations exhibits tails due only to high-energy multiplets. Charge transfer mixes the peaks due to $2p^5$-d^6 ionic multiplets and $2p^5$-$d^7\underline{L}$ satellites, smoothing the tails of the edges and leading to a better agreement with the spectra. The intensity ratio between the two L_2 peaks is not perfectly reproduced, the higher part being too intense compared to the lower-energy one. This discrepancy is also present in ionic calculations assuming perfect O_h symmetry.[10] It seems to be particular to d^5 ions as it does not happen in d^6 calculations (see FeO). At least our calculations show that it is not due to distortions from octahedral symmetry or charge transfer as both these phenomena are taken into account. We also checked that d orbital spin-orbit coupling cannot account for this discrepancy.

B. FeO

FeO presents a rocksalt structure. The thermodynamically stable structure contains iron vacancies corresponding to the approximate formulas $Fe_{1-x}O$ ($x \sim 0.1$). We have neglected the influence of vacancies and considered an FeO_6 cluster with perfect O_h symmetry to calculate iron $2p$ XAS in FeO, the iron ion being formally Fe^{2+}. The iron oxygen distance is 2.15 Å. To calculate Fe $2p$ XAS in FeO the parameters $\overline{r^2}$, $\overline{r^4}$, F^0_{dd}, F^0_{pd}, and η_σ were taken equal to those obtained for α-Fe_2O_3. The last parameter Δ_ϵ cannot be considered equal for α-Fe_2O_3 and FeO. Indeed ϵ_p and ϵ_d include not only the atomic energy of the p and d orbitals for the free ions but also the Madelung field on these orbitals. The Madelung fields in FeO and α-Fe_2O_3, assuming ionic charges on the ions can be found in Ref. 22. Due to the change in structure and iron valency, they are quite different in the two materials.

TABLE II. Parameters used the calculation of Fe $2p$ XAS.

$\overline{r^4}$	0.7 Å^4
$\overline{r^2}$	0.5 Å^2
F^0_{pd}	5.0 eV
F^0_{dd}	4.2 eV
η_σ	−1.0
Δ_ϵ (α-Fe_2O_3)	−25.5 eV
Δ_ϵ (FeO)	−28.0 eV

We had to assess Δ_ϵ for FeO. To do so, we considered iron $2p$ XPS in this material. The general shape of the spectra is close to the one of α-Fe_2O_3, but the satellites appear at 6 eV from the main peaks (8.2 eV in α-Fe_2O_3). This spectrum has been reproduced with $\Delta_\epsilon = -28$ eV and all other parameters kept constant. So we find a reduction of Δ_ϵ from α-Fe_2O_3 to FeO. This trend is in agreement with the calculated Madelung fields.[22] However due to the fact that they are calculated in ionic configuration the corresponding shift in Δ_ϵ is much larger than ours.

The configuration energy difference, including the calculated crystal field, is $\Delta = E(d^7\underline{L}) - E(d^6) = 4.0$ eV. Δ is larger in FeO than in α-Fe_2O_3 and, iron oxygen distances being larger in FeO, hopping terms are smaller for this oxide. Both these points lead to less important charge transfer in FeO than in α-Fe_2O_3 which can be seen in the smaller weight of the ligand hole ($d^7\underline{L}$) configuration (Table III). Moreover the larger iron oxygen distances make crystal-field splitting smaller in FeO ($10Dq = 0.73$ eV).

With this new set of parameters, we calculated iron $2p$ XAS for the FeO_6 cluster corresponding to FeO: the calculated spectrum show good agreement with the experimental one (see Fig. 2). Compared to α-Fe_2O_3 spectra, the occurrence of a single L_3 peak can be highlighted, as well as the symmetric shape of the L_2 edge. These features are characteristic of d^6 ions in an octahedral site. With close octahedral surroundings, the spectra for α-Fe_2O_3 and FeO are very different. The differences are due to the change in the number of occupations of the d orbitals (Formally d^5 and d^6 for Fe^{3+} and Fe^{2+}, respectively). Indeed it is known that the edge shape depends strongly on multiplet splitting of both ground-state formally d^n and final-state formally $2p^5$-d^{n+1} configurations. These multiplets are very different for d^5 to $2p^5$-d^6 and d^6 to $2p^5$-d^7 configurations which all have different possible spins and angular momentum. We can stress also that peak intensities relative to α-Fe_2O_3 are well reproduced without further intensity adjustment.

TABLE III. Charge-transfer results.

	$\Delta = E(d^{n+1}\underline{L}) - E(d^n)$ (eV)	Weight of $d^{n+1}\underline{L}$ configuration (%)
α-Fe_2O_3	2.2	40
FeO	4.0	20
Fe_3O_4 octahedral Fe^{3+}	2.2	45
Fe_3O_4 octahedral Fe^{2+}	3.9	30
Fe_3O_4 tetrahedral Fe^{3+}	2.2	35

Having satisfactorily interpreted the spectra of α-Fe_2O_3 and FeO we can deal with the case of structurally more complicated compounds.

C. Fe_3O_4

Fe_3O_4 is a mixed valence compound in which three different sites for iron ions exist. Their repartition is as follows: one-third are formally Fe^{2+} ions in octahedral symmetry, one-third are formally Fe^{3+} ions in octahedral symmetry, the remaining being formally Fe^{3+} in tetrahedral symmetry (see Table I for iron oxygen distances). So we had to consider three iron-oxygen clusters associated with each type of iron ion. We calculated the $2p$ XAS spectra for each of them. The Madelung fields of both Fe^{3+} sites being close to the one of iron in α-Fe_2O_3, we took the Δ_ϵ parameter of α-Fe_2O_3, for these two sites. Madelung fields of iron sites in FeO and Fe^{2+} in Fe_3O_4 are also nearly equal so that we took for this last site the Δ_ϵ parameter determined for FeO.[22] We first discuss these three spectra before tackling the calculation of the experimental spectra of Fe_3O_4 (see Fig. 3).

The spectrum of octahedral Fe^{3+} [Fig. 3(a)] is very close to the one obtained for the α-Fe_2O_3 cluster. The difference is only noticeable in L_3 peak intensity ratios. This difference is due to the change in iron-oxygen distances and distortions from O_h symmetry, the lattice being more important in Fe_3O_4 than in α-Fe_2O_3. On the contrary tetrahedral Fe^{3+} [Fig. 3(b)] and octahedral Fe^{2+} spectra are very different from the former two. The difference in surroundings for tetrahedral Fe^{3+} ions leads to different crystal field and charge transfer, the effect of which is a large reduction of the L_3 first peak and a different division of the L_2 edge which presents three peaks of growing intensity in the tetrahedral case. With exactly identical octahedral surroundings, the spectra for Fe^{3+} and Fe^{2+} ions [Fig. 3(c)] are also very different. This last spectrum can be compared with the one of FeO. The shape of the L_2 edge, which is quite symmetric, and the weakness of the L_3 first peak can be stressed. The noticeable differences come from the distortion of the Fe_3O_4 octahedral site, whereas in FeO the iron site has perfect O_h symmetry.

The values of the weights of the ligand hole ($d^{n+1}\underline{L}$) configurations are indicated in Table III. For octahedral Fe^{2+} it is smaller than for octahedral Fe^{3+}. The surroundings being identical, the crystal-field and hopping terms are equal on each site. The differences come therefore only from the greater value of Δ in the octahedral Fe^{2+} site. This is due to change in the d orbital occupation numbers and Madelung fields in the two sites.

At the opposite, even if Δ happens to be equal for tetrahedral and octahedral Fe^{3+}, the weight of ligand hole configurations on tetrahedral Fe^{3+} is smaller. This comes from a smaller amount of hopping for the tetrahedral site, the iron ion being surrounded by fewer neighbors.

Some quantitative analysis of the calculated spectra can be made. The area of the spectra are indicated in Table IV, the larger one being set to 1. These areas are proportional to the number of holes in the d orbitals in the ground state. This proportionality can be deduced from Fermi golden rule.[23] Our calculation indicates that this proportionality rule remains correct when charge transfer is considered. The branching ratio of the spectra is also indicated. They are very close to each other. The decrease from Fe^{3+} to Fe^{2+} is consistent with previous experimental and theoretical studies.[24]

In order to reproduce the spectrum of Fe_3O_4 the three spectra corresponding to the three clusters should be added in some way. The problem at this point is the relative energy position of the spectra. Taftø and Krivanek[7] found that the peaks coming from different sites appear at different energies. They indicated an ordering of the L_3 main peaks: starting from the lower energy should appear octahedral Fe^{2+}, tetrahedral Fe^{3+}, and octahedral Fe^{3+}, the tetrahedral Fe^{3+} peak lying in the middle of the other two. They proposed a value for the energy difference between the octahedral sites peaks of 1.3 eV. With our calculated spectra this value leads to a global shape that does not look like an experiment at all. In particular, experimentally, once the steps intensities are normalized the L_3 edge main line intensities for Fe_3O_4 and α-Fe_2O_3 are in a ratio about 75%. For a division of 1.3 eV the corresponding theoretical ratio is much smaller. In order to obtain the correct ratio we had to reduce the separation between the octahedral sites peaks to 0.7 eV, the tetrahedral site peak lying in the middle of them.

TABLE IV. Quantitative results on the calculated sites' spectra in Fe_3O_4.

	Fe^{3+} Octahedral	Fe^{2+} Octahedral	Fe^{3+} Tetrahedral
Branching ratio	0.748	0.731	0.751
$L_{2,3}$ edge area	0.979	0.791	1
Number of d in ground state holes	4.57	3.69	4.66

With this value the overall shape of the spectra is also in much better agreement with the experiment (see Fig. 3).

When compared to the α-Fe_2O_3 spectrum, the Fe_3O_4 spectrum [Fig. 3(d)] presents a weakening of the first peak of L_3 which appears only as a shoulder, a disappearance of L_2 splitting, and a global blurring of the spectrum. These trends are reproduced by our calculations. We already stressed the weakening of the L_3 first peak in both tetrahedral Fe^{3+} and octahedral Fe^{2+}. The change in L_2 edge shape is not perfectly reproduced, but the two peaks that can still be seen are much less resolved than in α-Fe_2O_3. This comes from a summation of three different looking spectra. The discrepancy for the higher-energy part of the spectrum that appeared in α-Fe_2O_3 is also visible for the Fe_3O_4 calculated spectrum. Still, our calculations account well for the differences in α-Fe_2O_3 and Fe_3O_4 spectra and confirm that they are due to the existence of three different types of cations in the latter material, the global spectra being the summation of the three associated spectra.

D. γ-Fe_2O_3

The case of γ-Fe_2O_3 is now considered. No experiment was made on γ-Fe_2O_3 in the present work. Experimental $2p$ EELS on this oxide can be found in Ref. 5. The experimental spectrum looks close to the one of α-Fe_2O_3. Nevertheless some differences can be seen in the L_3 edge shape. The intensity ratio between the L_3 first and main peaks seems larger in γ-Fe_2O_3 while the associated splitting is smaller. The experimental γ-Fe_2O_3 spectra is also blurred when compared to the α-Fe_2O_3 one.

In γ-Fe_2O_3 the formal valency of all iron ions is Fe^{3+}. Nevertheless there exist four different iron sites: in three of them iron ions are surrounded by six neighbors forming pseudo-octahedral surroundings and one is pseudotetrahedral (see Table I for iron-oxygen distances). Moreover the sites are not equally frequent in the material (see Table I). As for Fe_3O_4 we calculated the spectra of each site using α-Fe_2O_3 parameters, leading to four different spectra. The three pseudo-octahedral sites have, as expected, quite close spectra even if small differences can be seen [Figs. 4(b)–4(d)]. They come only from the different positions of oxygen atoms around iron leading to different distortions from O_h symmetry. An analysis of crystal-field splittings shows that the first octahedron is close to perfect O_h, while the second and third are more distorted. The spectra of the tetrahedral site looks close to the one of tetrahedral Fe^{3+} in Fe_3O_4 [Fig. 4(a)]. In lack of information about the way the different spectra are shifted, we can reasonably suppose that all the octahedral sites being close to each other, their spectra are aligned and consider only the shift of the tetrahedral one. We fitted this shift so as to reproduce, on the total spectrum, the experimental L_3 splitting of 1.35 eV indicated in Ref. 5. The corresponding shift is found to be 0.15 eV to the lower energies. The total calculated spectra is given in Fig. 4.

The differences between α-Fe_2O_3 and γ-Fe_2O_3 spectra are reproduced by our calculations [see Fig. 4(e)]. These differences in spectra can be attributed for a small part to pseudo-octahedral sites in γ-Fe_2O_3. But most of the differences come from the spectrum of the tetrahedral site as can be seen in Fig. 4. Once again the summation of the four spectra is responsible for the shape of the experimental spectrum. The blurring of the γ-Fe_2O_3 spectrum compared to α-Fe_2O_3 may be due to shifts in energy for

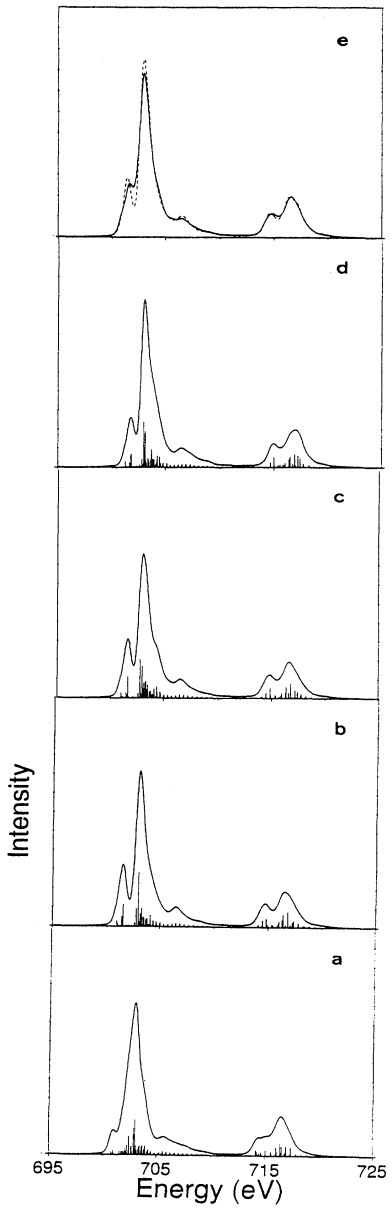

FIG. 4. Theoretical Fe $2p$ x-ray-absorption edge in γ-Fe_2O_3. (a) Theoretical spectrum and poles of the tetrahedral Fe^{3+} site. (b) Theoretical spectrum and poles of the first type of octahedral Fe^{3+} site. (c) Theoretical spectrum and poles of the second type of octahedral Fe^{3+} site. (d) Theoretical spectrum and poles of the third type of octahedral Fe^{3+} site. (e) The solid line is the theoretical γ-Fe_2O_3 spectrum obtained by weighted summation of (a)–(d). In the dashed line is figured the theoretical spectrum of α-Fe_2O_3 for comparison.

the different pseudo-octahedral sites which were not taken into account.

E. Insulating gap

The nature of the insulating gaps in transition-metal compounds has been a subject of research for a long time. In Ref. 11, Zaanen, Sawatzky, and Allen proposed a classification of transition-metal insulators in the so-called ZSA diagram. It involves two quantities Δ and U related to two elementary excitations. The charge-transfer energy Δ has already been defined, for a formally d^n compound as $\Delta = E(d^{n+1}\underline{L}) - E(d^n)$. U is the d-d charge fluctuation energy defined as

$$U = E(d^{n+1}) + E(d^{n-1}) - 2^* E(d^n) .$$

Depending on the relative values of U and Δ, the material is a Mott-Hubbard insulator ($U < \Delta$) or a charge-transfer insulator ($\Delta < U$). α-Fe_2O_3 is known to be a charge-transfer insulator.[25] The situation is less clear for FeO which is sometimes proposed to be a charge-transfer insulator[26] but is also suggested to enter the intermediate regime corresponding to nearly equal values.[24]

We can deduce from the parameters used in our calculations approximate values of U and Δ for the iron oxides and determine their position in the ZSA diagram. We already indicated the theoretical values of Δ. The values of U we shall use are for a d^5 ion in an octahedral field, $U = F^0_{dd} + \frac{2}{7}F^2_{dd} + \frac{2}{7}F^4_{dd} - 10Dq$; for a d^6 ion in an octahedral field, $U = F^0_{dd} - \frac{5}{49}F^2_{dd} + \frac{25}{441}F^4_{dd}$. α-Fe_2O_3 is indeed found to be a charge-transfer insulator as we find $\Delta = 2.2$ eV and $U = 9.5$ eV. For FeO we find $\Delta = 4.0$ eV and $U = 4.2$ eV. So we believe FeO to be in the intermediate regime, the difference between Δ and U being too small to allow a clear assignment to one type or the other.

In γ-Fe_2O_3, due to the different crystal-field splittings, the values of U and Δ are slightly varying among the sites; but the trend is the same as in α-Fe_2O_3. It is a charge-transfer insulator. In Fe_3O_4, one of the charge fluctuations, from octahedral Fe^{2+} to octahedral Fe^{3+}, corresponds to a formally zero-energy difference. It is known that conduction in Fe_3O_4 is due to these charge fluctuations,[27] making the ZSA classification ineffective for this compound.

V. CONCLUSIONS

Our approach proves able to calculate the $2p$ XAS spectral shapes of the different iron oxides: α-Fe_2O_3, FeO, Fe_3O_4, γ-Fe_2O_3. With a single set of parameters, except for Δ_ϵ, we succeed in reproducing and explaining the differences between these spectra. We found α-Fe_2O_3 and γ-Fe_2O_3 to be charge-transfer insulators and FeO to be in the intermediate regime. We trust this approach to be useful for all transition-metal compounds. The basic object we considered to account for cation $2p$ XAS spectra is the cation site, that is the cation with its close surrounding and its formal valency. We highlighted the strong effects of both valency and local deviation from perfect symmetry on spectral shape and pointed out the effect of charge transfer on spectra branching ratio and area.

ACKNOWLEDGMENTS

We would like to acknowledge G. Tourillon, C. Laffont, and P. Parent for technical support and advice during experiments on LURE. We are grateful to G. Dhalenne (from Laboratoire de Chimie du solide Orsay) for providing us magnetite and wüstite samples. Samples of hematite have been gracefully furnished by A. Cooper (from Bell Laboratories).

[1] R. L. Kurtz and V. E. Henrich, Phys. Rev. B **36**, 3413 (1987).
[2] M. Hendewerk, M. Salmeron, and G. A. Somorjai, Surf. Sci. **172**, 544 (1986).
[3] F. M. F. de Groot, J. C. Fuggle, B. T. Thole, and G. A. Sawatzky, Phys. Rev. B **42**, 5459 (1990).
[4] C. Colliex, T. Manoubi, and C. Ortiz, Phys. Rev. B **44**, 11 402 (1991).
[5] J. H. Paterson and O. L. Krivanek, Ultramicroscopy **32**, 319 (1990).
[6] R. D. Leapman, L. A. Grunes, and P. L. Fejes, Phys. Rev. B **26**, 614 (1982).
[7] T. Taftø and O. L. Krivanek, Phys. Rev. Lett. **48**, 560 (1982).
[8] G. van der Laan, M. P. Bruijn, J. B. Goedkoop, and A. A. MacDowell, Proc. Soc. Photo-Opt. Instrum. Eng. **733**, 354 (1987).
[9] P. Kuiper, B. G. Searle, P. Rudolf, L. H. Tjeng, and C. T. Chen, Phys. Rev. Lett. **70**, 1549 (1993).
[10] G. van der Laan and I. W. Kirkman, J. Phys. Condens. Matter **4**, 4189 (1992).
[11] J. Zaanen, G. A. Sawatzky, and A. W. Allen, Phys. Rev. Lett. **55**, 41 (1985).
[12] J. P. Crocombette and F. Jollet, J. Phys. Condens. Matter **6**, 8341 (1994).
[13] J. P. Crocombette and F. Jollet, J. Phys. Condens. Matter **6**, 10 811 (1994).
[14] R. D. Cowan, *The Theory of Atomic Structure and Spectra* (University of California Press, Berkeley, 1981).
[15] B. K. Teo and P. A. Lee, J. Am. Chem. Soc. **101**, 2815 (1979).
[16] J. C. Fuggle and J. E. Inglesfield, *Unoccupied Electronic States,* Topics in Applied Physics (Springer-Verlag, Berlin, 1992), Appendix B, p. 347.
[17] W. A. Harrison, *Electronic Structure and the Properties of Solids* (Freeman, San Francisco, 1980).
[18] J. S. Griffith, *The Theory of Transition Metal Ions* (Cambridge University Press, Cambridge, 1961).
[19] R. Wyckoff, *Crystal Structures* (Interscience, New York, 1964).
[20] C. Greaves, J. Solid State Chem. **49**, 325 (1983).
[21] J. Zaanen, C. Westra, and G. A. Sawatzky, Phys. Rev. B **33**, 8060 (1986).
[22] J. Q. Broughton and P. S. Bagus, J. Electron Spectrosc. Relat. Phenom. **20**, 261 (1980).
[23] B. T. Thole, P. Carra, F. Sette, and G. van der Laan, Phys. Rev. Lett. **68**, 1943 (1992).

[24]B. T. Thole and G. van der Laan, Phys. Rev. B **38**, 3158 (1988).
[25]A. Fujimori, M. Saeki, N. Kimizuka, M. Taniguchi, and S. Suga, Phys. Rev. B **34**, 7318 (1986).
[26]A. Fujimori, N. Kimizuka, M. Taniguchi, and S. Suga, Phys. Rev. B **36**, 6691 (1987).
[27]K. P. Belov, Usp. Fiz. Nauk **163**, 53 (1993) [Phys. Usp. **36**, 380 (1993)].